Cerebral Cortex, February 2018;28: 672–687

doi: 10.1093/cercor/bhx153
Advance Access Publication Date: 16 June 2017
Original Article

ORIGINAL ARTICLE

Experience-Dependent Regulation of Cajal–Retzius Cell Networks in the Developing and Adult Mouse Hippocampus

Max Anstötz[1,2], Sun Kyong Lee[1], Tamra I. Neblett[1], Gabriele M. Rune[2] and Gianmaria Maccaferri[1]

[1]Department of Physiology, Northwestern University, Feinberg School of Medicine, Chicago, IL 60611-3008, USA and [2]Institute for Neuroanatomy, University/University Hospital Hamburg, 20246 Hamburg, Germany

Address correspondence to Gianmaria Maccaferri, Department of Physiology, Feinberg School of Medicine Northwestern University, Chicago, IL 60611, USA. E-mail: g-maccaferri@northwestern.edu; Max Anstötz, Institute of Neuroanatomy, University Medical Center Hamburg-Eppendorf, 20245 Hamburg, Germany. Email: m.anstoetz@uke.de

Abstract

In contrast to their near-disappearance in the adult neocortex, Cajal–Retzius cells have been suggested to persist longer in the hippocampus. A distinctive feature of the mature hippocampus, not maintained by other cortical areas, is its ability to sustain adult neurogenesis. Here, we have investigated whether environmental manipulations affecting hippocampal postnatal neurogenesis have a parallel impact on Cajal–Retzius cells. We used multiple mouse reporter lines to unequivocally identify Cajal–Retzius cells and quantify their densities during postnatal development. We found that exposure to an enriched environment increased the persistence of Cajal–Retzius cells in the hippocampus, but not in adjacent cortical regions. We did not observe a similar effect for parvalbumin-expressing interneurons, which suggested the occurrence of a cell type-specific process. In addition, we did not detect obvious changes either in Cajal–Retzius cell electrophysiological or morphological features, when compared with what previously reported in animals not exposed to enriched conditions. However, optogenetically triggered synaptic output of Cajal–Retzius cells onto local interneurons was enhanced, consistent with our observation of higher Cajal–Retzius cell densities. In conclusion, our data reveal a novel form of hippocampal, cell type-specific, experience-dependent network plasticity. We propose that this phenomenon may be involved in the regulation of enrichment-dependent enhanced hippocampal postnatal neurogenesis.

Key words: BDNF, environmental enrichment, interneuron, neurogenesis, plasticity

Introduction

Cajal–Retzius cells are classically described as early-generated neurons, critically involved in the development of cortical networks (Frotscher 1998). In the neocortex, their densities dramatically decline during brain maturation to near-disappearance in adult animals (see review by Gil et al. 2014).

While 3 main hypotheses have been put forward regarding their vanishing, that is, dilution due to brain growth (Marin-Padilla 1990), transformation into a different neuronal type (Parnavelas and Edmunds 1983; Sarnat and Flores-Sarnat 2002), and cell death (Derer and Derer 1990), the latter proposal has received the strongest experimental support so far (Derer and Derer 1990; del Rio et al. 1995; Naqui et al. 1999; Tissir et al. 2009; Chowdhury et al. 2010; Anstötz et al. 2014, 2016; Ledonne et al. 2016).

Interestingly, recent work has also suggested that the molecular process(es) governing the death of Cajal–Retzius cells during brain development may be complex and involve both

lineage-specificity and local signals (Bielle et al. 2005; Ledonne et al. 2016). Although Chowdhury et al. (2010), Anstötz et al. (2014), and Ledonne et al. (2016) have all provided evidence for caspase-dependent apoptosis during the first postnatal weeks in the neocortex, the scenario may be different in the hippocampus, which is also mostly populated by cortical hem-derived Cajal–Retzius cells (Louvi et al. 2007; Gu et al. 2011). In fact, hippocampal Cajal–Retzius cells can be routinely observed in fully mature animals of several species (mice: Supèr et al. 1998; pigs: Abraham et al. 2004; humans: Abraham and Meyer 2003). The quantitative analysis performed in the CXCR4-EGFP reporter mouse (which allows the identification of Cajal–Retzius cells, see Marchionni et al. 2010) has suggested that the time-course of Cajal–Retzius cell decrease in the hippocampus is much slower compared with adjacent cortical areas (see Fig. 3 of Anstötz et al. 2016). Furthermore, in contrast to what observed in the neocortex, no evidence for caspase-dependent apoptosis of Cajal–Retzius cells was found in the hippocampus (Anstötz et al. 2016), suggesting that caspase-independent apoptotic processes may be involved. Consistently, neuronal apoptosis in the brain of caspase-3 and caspase-9 knockout mice displays a delayed onset compared with wild-type animals (Oppenheim et al. 2001), and recent work has shown that the death of cortical hem-derived Cajal–Retzius cells does not require the proapoptotic factor Bax (Ledonne et al. 2016)

Thus, the apparent unique developmental regulation of Cajal–Retzius cell number in the hippocampal circuit suggests the intriguing possibility that this may be related to similarly unique hippocampal features, which may require the persistence of Cajal–Retzius cells in the fully mature network. For example, compared with other cortical areas, a specific property of the dentate gyrus of the hippocampus is its continuous ability to sustain neurogenesis even during adulthood (see review by Aimone et al. 2014).

From a circuit standpoint, the synaptic integration of newborn granule cells is a complex process, heavily regulated by GABAergic input (Tozuka et al. 2005) received from local interneurons (e.g., neurogliaform and parvalbumin-expressing interneurons: Markwardt et al. 2011; Song et al. 2013). Both the location and distribution pattern of the axonal arborization of Cajal–Retzius cells along the hippocampal fissure and in the outer molecular layer of the dentate gyrus (Anstötz et al. 2016) suggest their potential involvement in controlling GABAergic interneuronal populations that target the neurogenic niche. More importantly, both the optogenetic activation of Cajal–Retzius cells and direct paired recordings have established that Cajal–Retzius cells can synaptically excite various types of interneurons, including neurogliaform cells, via glutamatergic transmission (Quattrocolo and Maccaferri 2014; Anstötz et al. 2016). In addition, Cajal–Retzius cells are a source of the chemokine C-X-C motif chemokine ligand 12 (CXCL12, also known as SDF1, see Bagri et al. 2002), which is believed to tonically activate CXC chemokine receptor 4 (CXCR4) in immature granule cells and to be essential for the correct regulation of adult neurogenesis (Kolodziej et al. 2008).

Thus, assuming a role of Cajal–Retzius cells in the proliferation/maturation of newborn granule cells, we hypothesized that experimental conditions enhancing hippocampal neurogenesis should also be associated with an increased persistence of Cajal–Retzius cell networks in the hippocampus, but not in other cortical areas. Here, we have taken advantage of multiple mouse reporter lines, which allow the identification of Cajal–Retzius cells, to directly test this possibility. Our results show that environmental enrichment can dynamically regulate the density of hippocampal Cajal–Retzius cells and provide an important experimental evidence for a novel form of cell type-specific, experience-dependent, plasticity in the hippocampus.

Materials and Methods

Ethical Approval

All experimental procedures used in this study were approved by the Institutional Animal Care and Use Committee of Northwestern University and are in compliance with animal guidelines provided by the National Institutes of Health.

Animals

Both male and female reporter animals were used. Mice were generated by breeding either Wnt3a-IRES-Cre (strain: B6(Cg)-*Wnt3a*$^{tm1.1(cre)Mull}$/Mmmh, stock number: 031748-MU, see Gil-Sanz et al. 2013) or PDE1c-Cre BAC transgenic mice (strain: B6.FVB(Cg)-Tg(Pde1c-cre)IT146Gsat/Mmucd, stock number: 036699-UCD) with a line that conditionally expresses the tdTomato fluorescent protein following Cre-dependent removal of a floxed STOP cassette (from Jackson Laboratory, strain: B6.Cg-Gt(ROSA)26Sor$^{tm9(CAG-tdTomato)Hze}$/J, stock number: 007909, also known as Ai9). Henceforth, we will refer in the text and in the figures to the resulting tdTomato-expressing animals either as Wnt3a or PDE1c, respectively.

For electrophysiological experiments requiring optogenetic stimulation of Cajal–Retzius cells (Quattrocolo and Maccaferri 2014), we bred Wnt3a-IRES-Cre mice with a strain that conditionally expresses an improved channelrhodopsin-2(ChR2)-EYFP (enhanced yellow fluorescent protein) fusion protein (ChR2[H134R]-EYFP) following Cre-mediated removal of the floxed STOP cassette (from Jackson Laboratory, strain, B6;129S-Gt[ROSA]26Sortm32[CAG-COP4*H134R/EYFP]Hze/J; stock number: 012569, see Madisen et al. 2012). For simplicity, we will refer to the offspring of this crossing as Wnt3a-ChR mice.

Environmental Enrichment

Control mice were housed under standard condition (igloos), whereas running-wheel-igloo enrichments (BioServ, Flemington, NJ, USA) were included in cages of treated mice. Furthermore, Enviro-Dri (Shepherd Specialty Papers, Watertown, TN, USA) was also added in the environmental enriched group in order to promote more physiological nesting behavior.

Histological Analysis

Mice of different genotypes and ages were used for immunohistochemical experiments. Animals were anesthetized by intraperitoneal injection of sodium pentobarbital (270 mg/kg body weight) and perfused with isotonic saline followed by 4% formaldehyde in 0.12 M phosphate buffer (PB), pH 7.4. After perfusion, brains were extracted from the skulls, and cryoprotected in 30% sucrose in PBS. Hippocampal sections were cut serially at 60 µm on a freezing-stage microtome. Immunocytochemical reactions were carried out as follows.

TdTomato Immunocytochemistry

Fixed brain sections were pretreated in TBS containing 10% methanol and 0.3% H_2O_2 for 30 min at RT, followed by rinses in TBS. TBS containing 5% normal goat serum (NGS), 1% bovine serum albumin (BSA) and 0.2% triton X-100 was used for blocking the reaction for 1 h at RT. Sections were then incubated overnight with primary antibody recognizing TdTomato

(1:3000, rabbit; catalog# 632496 [Clontech Laboratories Inc, Mountain View, CA, USA]) at 4°C. After washing in TBS, a secondary antibody conjugated to biotin (1:500, donkey; catalog# RPN-1004V-2ML [GE Healthcare Life Sciences, Pittsburgh, PA, USA]) was applied to enhance immunoreactivity signals. Biotinylated sections were processed through an avidin/biotin amplification reaction using the Elite ABC Vectastain Kit (catalog# PK-6100, Vector Laboratories, Burlingame, CA, USA) and 3,3′-diaminobenzidine (DAB) as chromogen to stain tdTomato-expressing Cajal–Retzius cells. All sections were finally mounted in Mowiol (catalog# 10981, Sigma-Aldrich Corp., St. Louis, MO, USA) and analyzed under the microscope as described below.

Ki-67 and Parvalbumin Immunocytochemistry

Brain sections were prepared from Wnt3a and PDE1c P36 animals from both control and environmental enriched groups. Fixed sections were pretreated in TBS containing 5% NGS, 1% BSA and 0.2% Triton X-100 for 1 hr at RT. Anti-Ki-67 (1:1000, rabbit; catalog# RM-9106-S0 [Thermo Fisher Scientific, Waltham, MA, USA]) and anti-Parvalbumin (1:1000, mouse; catalog# PV235[SWANT]) primary antibodies were applied in TBS containing 1% NGS, 1% BSA and 0.2% Triton X-100 at 4°C overnight. Secondary antibodies coupled to Alexa647 (1:500, goat; catalog# A21244 [Life Technologies, Carlsbad, CA]) and Alexa488 (1:500, goat; catalog#A11001 [Life Technologies]) were used to visualize Ki-67 and Parvalbumin antibodies, respectively. After the secondary antibody reaction, DAPI (catalog# 62249, Life Technologies) was applied during the initial wash in TBS. Processed sections were coverslipped with Mowiol mounting medium and analyzed under a confocal microscope.

Reelin and Calretinin Immunocytochemistry

We used the same general procedure described above for Ki67 and Parvalbumin. Primary antibodies were: anti-reelin antibody (1:1000, mouse; catalog# MAB5364 [Millipore]) and anti-calretinin antibody (1:1000, rabbit; catalog# CR7697 [SWANT]). Secondary antibodies to reveal reelin were coupled to Alexa488 (1:500, goat; catalog#A11001 [Life Technologies]), whereas for calretinin labeling, coupling was to Alexa647 (1:500, goat; catalog# A21244 [Life Technologies]).

Brightfield and Fluorescence Microscopy

Common brightfield and fluorescence microscopic images were obtained using a Kyence BX-9000 and a Zeiss AxioScope 2 FS. For Extended Focal Imaging, multiple z-stacks were obtained and in-focus areas merged in Adobe Photoshop.

For the combination of brightfield with fluorescent images, the monochromatic brightfield-image image was inverted and a green LUT was applied. Confocal microscopy images were captured using a Leica SP5 with HyD detectors. Single- or multichannel fluorescence images were saved individually for analysis and merged together for colocalization studies and figures using Adobe Photoshop.

Analysis of Immunohistochemical Colocalization

Confocal microscopy image-stacks were captured using a Leica SP8 with HyD detectors. For the analysis of protein co-expression of stained neurons, z-stacks with 2 µm interval were taken with a Leica 63 × 1.4 NA lens resulting in a digital resolution of at least 180 nm/pixel and a captured area of 17 000 µm^2 (183 by 92 µm). Using a line histogram drawn through a single neuron in Leica LAS AF Lite software, the fluorescence intensities in all channels (for DAPI, tdTomato, calretinin, and reelin) were measured.

Quantification of the Density of Cajal–Retzius cells, Parvalbumin-Stained Neurons, and Ki-67 Immunopositive Nuclei

This analysis was carried out using a procedure similar to what described in Anstötz et al. (2016). Briefly, Wnt3a and PDE1c mice aged P7, P14, P21, P30, P36, and P112 were prepared as described above. Counting was performed on $n = 6$ sections per mouse (60 µm thick horizontal slices). For each age and treatment group, $n = 3$ animals were evaluated resulting in a total of 18 sections for each developmental age within a specific treatment.

For the quantification of Cajal–Retzius cells, z-stacks with 4 µm interval were taken using a Kyence BX-9000 microscope with a Nikon Apo 20 × 0.75 NA lens or a Zeiss AxioScope with a 2 FS 20x resulting in a digital resolution of at least 550 nm/pixel. Each z-stack was analyzed individually using a NEUROLUCIDA-based station and software (MicroBrightfield; Williston, VT, USA). Cajal–Retzius cells were marked and layer borders outlined. Cajal–Retzius cells could be easily identified by their tdTomato expression, typical "tadpole" like shape, and localization in the hippocampal molecular layers/L1. Two regions of interest were defined: the hippocampus (Hip) and the adjacent cortex (L1). These regions were defined by outlining the border of the dentate gyrus and the pial surface of layer 1 in the adjacent cortex respectively. Cell density was calculated as a line-density for each region. In the case of parvalbumin-positive cells, we calculated both linear- and area-densities by measuring the number of immunostained cells per linear length of inner granule cell layer (GCL) and area of the dentate gyrus. As both quantifications yielded the same result (i.e., no difference in densities in control vs. treated animals), we present in the figure linear density summary plots for consistency.

For the quantification of dividing neurons, z-stacks with 4 µm interval were taken and analyzed as described above. Proliferating cells in the subgranular zone (SGZ) were identified by the colocalized expression of DAPI and Ki67. The number of Ki67 positive nuclei in the SGZ was normalized by the length of the inner GCL for each section.

Generation of Spatial Density Plots

2D maps of Cajal–Retzius cell densities were constructed using the raw data obtained by NEUROLUCIDA containing the exact spatial information of counted cells. The absolute spatial information of every Cajal–Retzius cell was converted into a relative position using hippocampal fix-points (pole and split-point of the hippocampal fissure; medial and lateral curvature of the dentate gyrus; pial ending of the infrapyramidal blade of the dentate gyrus). These normalized positions were plotted into a scheme of a representative hippocampal formation. The absolute numbers of Cajal–Retzius cells were measured in a 50 × 50 µm^2 Cartesian grid, yielding a raw density map. The data of "region-specific density" plots were processed and visualized as a Contour-Plot with bicubic interpolation in Mathematica 7 (Wolfram Research, Champaign, IL, USA). The lower bound of the scale was set to 0, the upper bound to the maximum density (in the examined age). Difference plots were simply obtained by subtracting the raw density maps.

Electrophysiological Methods

Acute hippocampal slices were prepared as follows. First, animals were deeply anesthetized with isoflurane and then decapitated. The brain was gently removed and bathed in a chilled modified artificial cerebrospinal fluid (ACSF, in mM): 130 NaCl,

24 $NaHCO_3$, 3.5 KCl, 1.25 NaH_2PO_4, 1 $CaCl_2$, 2 $MgSO_4$, 10 glucose, saturated with 95% O_2, 5% CO_2 (pH = 7.4). A vibratome microtome (Leica VT 1200 S) was used to cut transverse sections (350 µm thickness), which were then incubated at 34–35°C for about 30 min and then stored at room temperature. When required, slices were transferred to a direct microscope (Olympus BX-51) with oblique illumination optics and an infrared camera system (Zyla 4.2, Andor Technology, Belfats, UK). Cells were first identified as tdTomato-expressing under using a 60x IR water immersion objective and a LED (520 nm wavelength) light source (Prizmatix, Jerusalem, Israel). Slices were superfused with preheated ACSF of the following composition (in mM): 130 NaCl, 24 $NaHCO_3$, 3.5 KCl, 1.25 NaH_2PO_4, 2 $CaCl_2$, 1 $MgSO_4$, 10 glucose, saturated with 95% O_2, 5% CO_2 (pH = 7.4) and maintained at a constant temperature (29–31°C) by a temperature controller (TC-324B, Warner Instruments, Hamden, CT, USA). Electrodes were pulled from borosilicate glass capillaries (Prism FLG15, Dagan Corporation, Minneapolis, MN, USA) and had a resistance of 3–5 MΩ when filled with the appropriate internal solution, as reported below. Recordings were performed using a Multiclamp 700 amplifier (Molecular Devices, Sunnyvale, CA, USA). Analog signals were filtered at 3 KHz and digitized at 50 kHz using a Digidata 1322 A and the Clampex 9 program suite (Molecular Devices). Access resistance was compensated in current-clamp configuration with a bridge circuit and membrane input resistance was estimated by the slope of the I/V plot built from the injection of four 1 s long negative current steps (–5 to –20 pA in 5 pA steps) from cells held at ~–60 mV.

Optogenetic experiments were performed on age-matched (P23, P24, and P25) Wnt3a-ChR animals housed either in standard ($n = 4$) or environmental enriched conditions ($n = 4$). Blue light was transmitted to the slice from a collimated LED (Prizmatix) attached to the epifluorescence port of a direct microscope. The light flash (1 ms duration, relative intensity 1.5) was pointed to the soma of the recorded interneuron via a mirror coupled to a 60x objective (1.0 numerical aperture). Analysis of the synaptic responses was performed using the Clampex 9 program suite. Measurements were obtained from averages of 5 responses obtained with an interstimulus interval of 30 s. The estimated series resistance of the recordings was not different in the control versus environmental enriched groups (25 ± 1 MΩ, $n = 22$ vs. 24 ± 1, $n = 21$, $P > 0.05$).

Pipette Solutions

Current-clamp recordings from Cajal–Retzius cells were performed using the following intracellular solution (in mM): 125K-methylsulfate, 10 NaCl, 0.3 GTP-Na, 4 ATP-Mg_2, 16 KHCO3, and 0.3–0.5% biocytin, equilibrated with 95% O_2, 5% CO_2 (pH = 7.3) and 0.2–0.4% biocytin. Voltage-clamp recordings from interneurons used pipettes filled with the following solution: 125 Cs-methanesulfonate, 0.3 GTP-Na, 4 ATP-Mg_2, 16 $KHCO_3$, 10 QX314-Cl, and 0.2–0.4% biocytin, equilibrated with 95% O_2, 5% CO_2 (pH = 7.3).

Recovery of Biocytin-Filled Cells and Reconstructions

Biocytin-filled neurons were fixed in 4% paraformaldehyde in 0.1 M PB at 4°C for at least 24 h. Endogenous peroxidase activity was quenched with a 3% H_2O_2 solution for 15 min. Sections were incubated overnight at 4°C in avidin-biotinylated-HRP complex (Vectastain ABC Elite kit) with 0.1% Triton X-100 in PB, followed by a peroxidase reaction with DAB tetrahydrochloride as a chromogen. Cells were revealed by adding 0.025%, and the reaction was stopped when dendritic and axonal processes were clearly visible under light microscopy examination. After several washing steps in 0.1 M PB, slices were postfixed with 0.1% OsO_4 in PB (1–2 min), and then mounted on slides with Mowiol (Hoechst AG, Frankfurt AM, Germany). Cells were reconstructed using a using a NEUROLUCIDA-based station and software. Post hoc biometric data were generated by NERUOLUCIDA Explorer software. Sholl analysis was performed with a 50 µm starting radius and a 50 µm interval.

Statistical Methods

Statistics were performed using a Mann–Whitney *U* test comparing 2 groups (single or 2 tailed as appropriate, Motulsky 2010) or 2-way ranked ANOVA comparing multiple groups/categories with LSD post hoc tests (Saville 1990) in IBM SPSS Statistics Ver. 22 (IBM Corp, Armonk, NJ, USA). Level of significance for individual tests was chosen as $P < 0.05$. Values in the text are given as mean ± standard error. Box plots in the illustrations indicate the median (middle dash), the lower and upper quartile (box borders), and minimum and maximum values (whiskers). Sholl analysis plots are displayed as mean ± standard error.

Results

The quantification of Cajal–Retzius cell numbers in the postnatal hippocampus is a difficult process that may suffer from limitations depending on the technique used. For example, immunohistochemical identification relying on specific molecular markers such as reelin or calretinin is not exclusive for Cajal–Retzius cells, as both reelin- and calretinin-expressing interneurons have been described in the molecular layers of the hippocampus (Gulyás et al. 1996; Pesold et al. 1998; Fuentealba et al. 2010). In addition, hilar mossy cells, which target the dentate gyrus inner molecular layer, also show calretinin immunoreactivity in mice (Blasco-Ibáñez and Freund 1997). Furthermore, the expression of these molecular markers has been reported to be developmentally down-regulated (Ringstedt et al. 1998; Coppola et al. 2015), thus potentially leading to the underestimation of Cajal–Retzius cell persistence in adult tissue.

Although, as an alternative approach, the use of BAC transgenic reporter mice (e.g., Ebf2-EGFP, Chowdhury et al. 2010, and CXCR4-EGFP, Anstötz et al. 2014, 2016) may allow an easy appreciation of the typical “tadpole-like” neuronal morphology of Cajal–Retzius cells, this technique also suffers from the unverified assumption that the specific promoters that drive the expression of the reporter molecules are not developmentally modulated. In order to avoid these potential caveats, we decided to take advantage of Cre-loxP recombination (Nagy 2000). Specifically, we used 2 mouse lines that express Cre recombinase under the control of the Wnt3a and PDE1c genes, which are both active at embryonic stages in Cajal–Retzius cells (Osheroff and Hatten 2009; Gil-Sanz et al. 2013), and crossed them with reporter tdTomato floxed animals (Ai9, see Materials and Methods). Henceforth, we will refer in the text and in the figures to the resulting tdTomato-expressing animals either as Wnt3a or PDE1c, respectively. In both cases, as shown in Figure 1, hippocampal Cajal–Retzius cells could be identified both by their typical tadpole-like morphology and by their location in the molecular layers (stratum lacunosum-moleculare of the hippocampus proper and the outer molecular layer of the dentate gyrus). Non-Cajal–Retzius cells were also occasionally labeled (as previously reported in Quattrocolo and Maccaferri 2014),

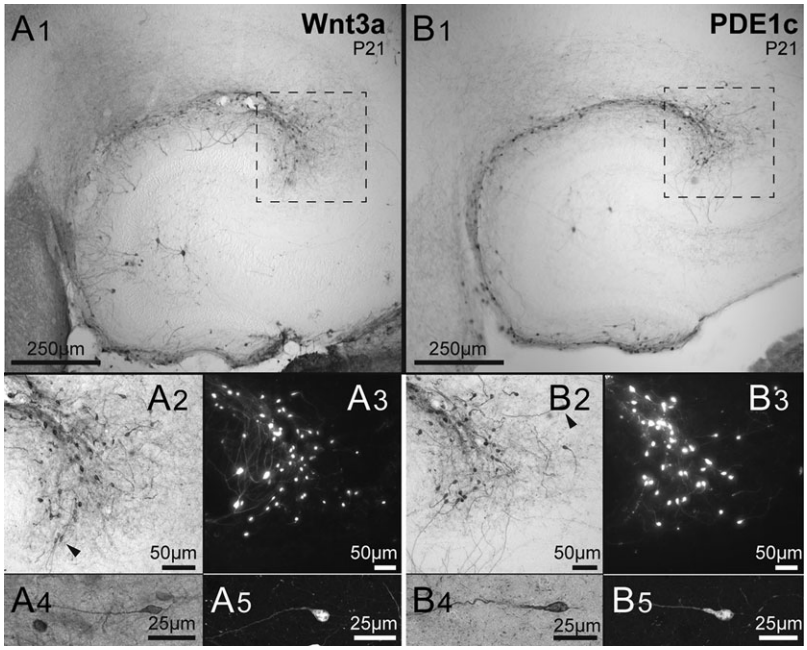

Figure 1. Two lines of tdTomato reporter mice identify Cajal–Retzius cells. (*A1*) Low-magnification micrograph of immunolabeled cells of the Wnt3a mouse hippocampus. Notice the presence of cells along the hippocampal fissure and dentate gyrus outer molecular layer. As previously reported (Quattrocolo and Maccaferri 2014) notice also the presence of a few stained granule cells and hilar neurons. The dotted square identifies the CA3 pole region, which has the highest density of Cajal–Retzius cells (Anstötz et al. 2016). (*A2*,*A3*) Cajal–Retzius cells of the pole region shown at higher magnification in a DAB stained slice (dotted region of *A1*) and in a different preparation with fluorescence microscopy. Individual cells are shown in more detail in the (*A4*,*A5*) panels. Notice the typical "tadpole" morphology identifying the neurons as a Cajal–Retzius cells. (*B1*–*B5*) Sections obtained from PDE1c mice. Notice the clear labeling of Cajal–Retzius cells. Same organization as in (*A1*–*A5*).

but could be easily distinguished both by their location outside the molecular layers and by their obvious non-Cajal–Retzius cell-like appearance.

In both Wnt3a and PDE1c mouse lines, labeled Cajal–Retzius cells expressed reelin and calretinin, as expected (Fig. 2). We found reelin immunoreactivity in 100% of tdTomato-expressing neurons of the molecular layers of both Wnt3a (n = 211 cells, P36) and PDE1c mice (n = 144 cells, P36), whereas calretinin was expressed in the majority, but not in all tdTomato-positive cells (89% in Wnt3a and 92% in PDE1c mice, respectively). This latter finding is consistent with reports that not all Cajal–Retzius cells express calretinin (Bielle et al. 2005). In addition, as previously mentioned, neither reelin nor calretinin staining was exclusive for Cajal–Retzius cells, as these molecular markers were also found in mossy cells and interneurons (Fig. 2). In fact, calretinin-immunoreactivity in the absence of tdTomato labeling was observed consistently at the level of axonal arborizations in the inner molecular layer (and in the cell bodies of putative hilar mossy cells originating these axons), but extremely rarely in neurons with somata located in the molecular layers (Wnt3a mouse: 0% out of a total of 187 cells, and PDE1c mouse: 2% out of a total of 118 cells). However, we could also find a substantial minority of reelin-immunoreactive cells that were not labeled by tdTomato, (Fig. 2, Wnt3a mouse: 18% out of a total of n = 258 cells, PDE1c mouse: 20% out of a total of 181 cells). These cells are likely to be reelin-expressing neurogliaform interneurons (Fuentealba et al. 2010), which are abundant in the hippocampal molecular layers (see recent review by Overstreet-Wadiche and McBain 2015). Lastly, No changes in the pattern of immunostaining were revealed when the same procedures were applied to slices obtained from either Wnt3a or PDE1c mice of the same age (P36) exposed to enriched conditions (data not shown).

We further corroborated our conclusion that tdTomato labeling in the molecular layers was restricted to Cajal–Retzius cells by performing electrophysiological recordings (from young animals, n = 5 mice, range: P13–P16), as shown in Figure 3. In a total of 26 tdTomato-expressing cells recorded (n = 16 Wnt3a and n = 10 PDE1c animals exposed to enriched conditions) we observed the typical firing patterns and membrane hyperpolarizing responses previously described for hippocampal Cajal–Retzius cells (von Haebler et al. 1993; Marchionni et al. 2010, 2012; Quattrocolo and Maccaferri 2013, 2014; Anstötz et al. 2016). The estimated membrane input resistance was 2.0 ± 0.2 and 2.3 ± 0.1 GΩ for Wnt3a and for the PDE1c genotypes, respectively (P > 0.05). In n = 15 and 6 anatomically recovered cells (Wnt3a and PDE1c strain, respectively) we could successfully examine the morphology of the biocytin-filled neurons, which were, in all cases, Cajal–Retzius cells.

Thus, having experimentally confirmed that these 2 animal lines are appropriate for the identification of Cajal–Retzius cells, we decided to use them to compare their densities during development in 2 mouse groups housed under different conditions: control and environmentally enriched (see Materials and Methods for details).

As shown in Figure 4, environmental enrichment caused a significant increase of Cajal–Retzius cell density (measured as number of cells per 100 µm of hippocampal fissure, see Materials and Methods and Anstötz et al. 2016 for details) from 5.9 ± 0.2 to 7.7 ± 0.3 (in Wnt3a animals, P < 0.001) and from 6.3 ± 0.2 to 7.4 ± 0.4 (in PDE1c mice, P < 0.05) at a juvenile developmental stage (P36). In contrast, Cajal–Retzius cells of layer 1 of the adjacent cortex were not affected by environmental enrichment. Their densities (measured as cells per 100 µm of layer 1, see Materials and Methods and Anstötz et al. 2016 for details) displayed similar values of 1.5 ± 0.2 to 1.6 ± 0.2 (control vs.

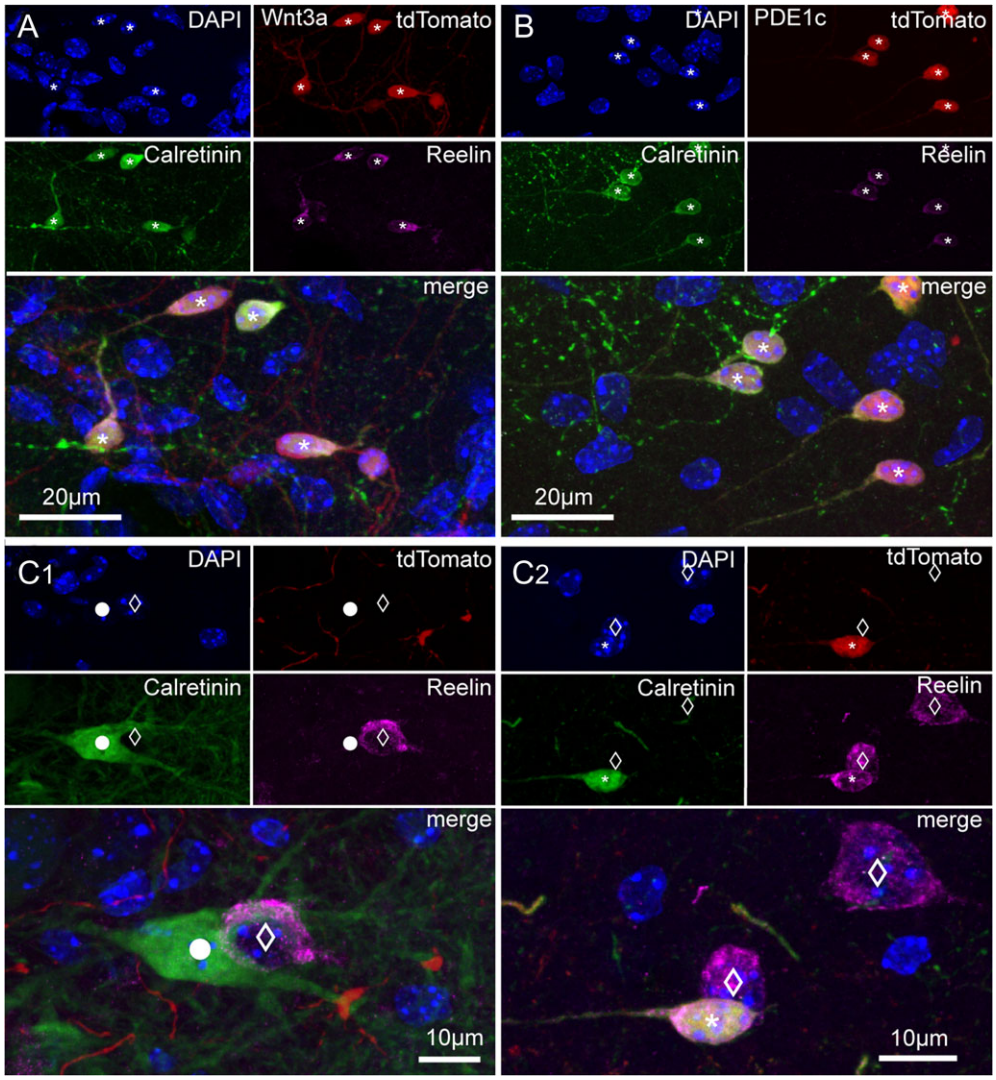

Figure 2. Immunoreactivity for calretinin and reelin in tdTomato-positive and negative cells of Wnt3a and PDE1c animals. (*A*) Images of the hippocampal fissure region from a juvenile Wnt3a mouse (P36) showing DAPI nuclear counterstaining and the labeling of tdTomato, calretinin, and reelin in single pictures, and then superimposed. Cells identified by the asterisks express all markers. (*B*) As in (*A*), but for the PDE1c mouse line (P36). (C1,C2) Calretinin and reelin immunoreactivity in cells that do not express tdTomato. (C1) Calretinin labeling of a putative hilar mossy cells (circle) and reelin positivity of a putative hilar GABAergic interneuron (empty diamond). DAPI nuclear counterstaining, tdTomato, calretinin, reelin labeling shown first as isolated images, and then superimposed. (C2) Reelin immunoreactivity in cells non expressing tdTomato in the hippocampal fissure region. DAPI nuclear counterstaining, tdTomato, calretinin, and reelin labeling of cells of the hippocampal molecular layers are first shown as single pictures and then superimposed. Notice the nontadpole-like morphology of the 2 reelin-positive cells (empty diamonds) that are not labeled by tdTomato and the tadpole-like appearance of the tdTomato, reelin, and calretinin-expressing cell (asterisk).

enrichment, respectively, Wnt3a animals, $P > 0.05$) and 1.9 ± 0.1 to 2.2 ± 0.2 (control vs. enrichment, respectively, PDE1c mice, $P > 0.05$).

We also verified, in the same slices, that enhanced environmental conditions were effective in increasing dentate gyrus neurogenesis. When we quantified the density of nuclei stained for the protein Ki67 per 100 µm of inner GCL length (Ki67 is considered a useful marker of neurogenesis, see Kee et al. 2002), we observed a significant increase in the treated group. In Wnt3a mice 7.4 ± 0.3 nuclei per 100 µm were Ki67 immunopositive in control compared with 9.8 ± 0.4 in enriched conditions ($P < 0.001$). Similar results were obtained in PDE1c animals (from 5.6 ± 0.3 Ki67-stained nuclei per 100 µm in the control vs. 7.8 ± 0.5 in the treated group, $P < 0.001$).

In order to corroborate the idea that the impact of environmental enrichment on Cajal–Retzius cells is due to cell-type specific mechanisms, and not to global effects involving every type of neuron, we compared the densities of dentate gyrus parvalbumin-immunoreactive interneurons in juvenile mice (P36) housed in control versus enhanced conditions (Fig. 5). As shown in Figure 5, the density of parvalbumin interneurons (measured as number of parvalbumin-labeled interneurons per 100 µm of inner GCL) was not affected either in Wnt3a or PDE1c animals. In Wnt3a control mice the density of parvalbumin cells was 1.72 ± 0.12 compared with 1.71 ± 0.09 in the group exposed to environmental enrichment ($P > 0.05$). Similarly, in PD1Ec animals densities were 2.34 ± 0.07 and 2.56 ± 0.10 in control versus treated animals ($P > 0.05$). However, we also confirmed in the same mice that exposure to enriched conditions increased the density of Ki67-stained nuclei (Wnt3a from 7.66 ± 0.27 to 8.94 ± 0.37, $P < 0.05$ and in PDE1c from 7.54 ± 0.35 to 9.28 ± 0.49, $P < 0.01$).

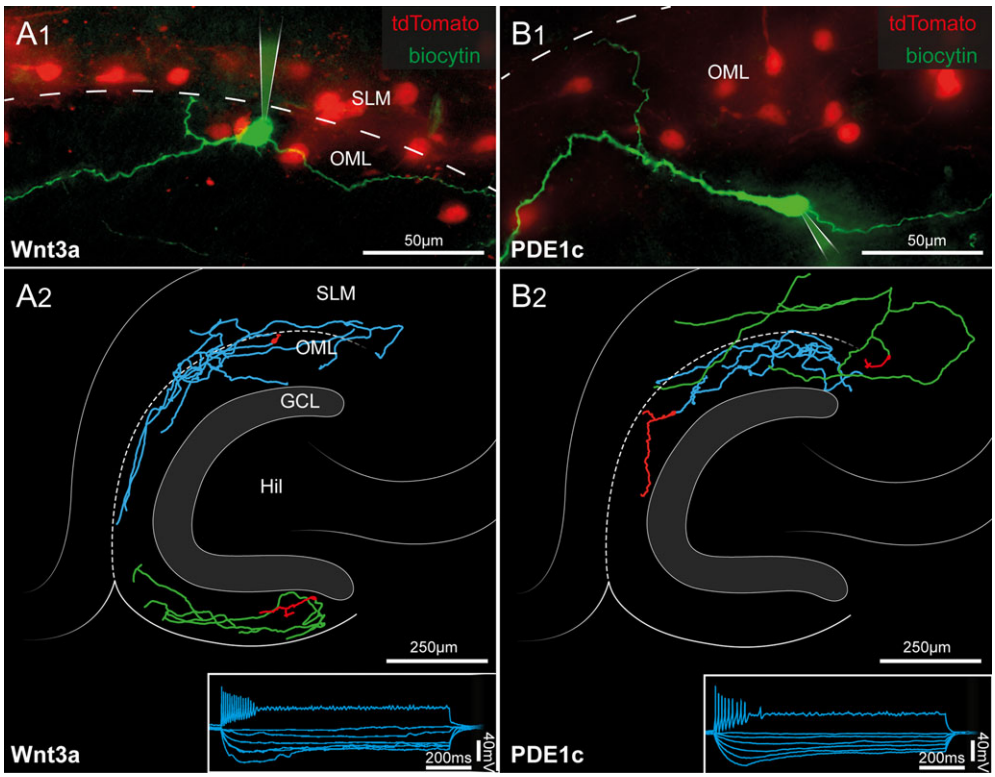

Figure 3. Morphofunctional identification of tdTomato-expressing cells of the hippocampal molecular layers as Cajal–Retzius cells. (*A1*) Pseudo-color image showing a biocytin-filled Cajal–Retzius cell (green) in a slice obtained from a P15 Wnt3a mouse. Notice the typical emergence of the axon (arrowhead) opposite the main dendritic trunk. Remaining tdTomato cells are shown in red. SLM, stratum lacunosum-moleculare; OML, outer molecular layer of the dentate gyrus. The dotted line marks the hippocampal fissure. (*A2*) Post hoc anatomical reconstructions of 2 recorded Cajal–Retzius cells form Wnt3a mice. Notice the typical axonal arborization in the hippocampal molecular layers and the lack of a complex dendritic tree. Hil, hilus; GCL, granule cell layer. The bottom right inset shows the electrophysiological response of a labeled cell to a series of current steps (1 s duration, −25, −20, −15, −10, −5, and 65 pA). (*B1*,*B2*) Same experiments and analysis as in (*A1*,*A2*), performed on slices from P13 PDE1c mice.

Having verified the effectiveness of our treatment in juvenile animals, we next decided to investigate the time-course of the impact of environmental enrichment on Cajal–Retzius cells in mice from early postnatal ages to full adulthood.

As shown in Figure 6, we found that the effect of enriched conditions was measurable as an overall increase of hippocampal Cajal–Retzius cell densities ($P < 0.001$), with significant increases in the P21–P112 range. In Wnt3a mice we estimated a relative augmentation of ~30% for animals older than P14, which was similar to what calculated for PDE1c animals (~23%). No change was observed at younger ages (1% and −1% in the 2 aforementioned genotypes, respectively, P7–P14,). Cajal–Retzius cells in layer 1 of the adjacent cortex did not show any differences between controls and treated groups (~7% and ~3% relative increase for the entire P7–P112 range in Wnt3a and PDFE1c, respectively, $P > 0.05$ in both cases). Another interesting observation from these experimental datasets is that the density of Cajal–Retzius cells of the fully mature hippocampus (P112) is similar to what estimated in the adjacent cortical areas at much earlier postnatal stages (P7–P14). Taken together, these results unequivocally confirm previous suggestions that not only are Cajal–Retzius cells present in the developing hippocampus, but they are also an integral part of its adult circuits.

We next investigated whether the effect of the treatment was specific to particular subfields of the hippocampus or it was homogeneously distributed. As shown in Figure 7, density plot maps revealed a broad effect distributed to all the molecular layers along the hippocampal fissure and in the outer molecular layer of the infrapyramidal blade of the dentate gyrus. Thus, the impact of environmental enrichment appears to generally affect the density of hippocampal Cajal–Retzius cells, irrespective of their specific subfield localization.

Although the typical morphology of Cajal–Retzius cells could be easily distinguished in processed sections from older animals, we decided to further corroborate this finding in order to rule out the possibility that tdTomato-expressing cells observed in the molecular layers of fully mature animals were the result of Cre-loxP recombination occurring at adult stages in non-Cajal–Retzius cell types. We performed electrophysiological recordings in slices obtained from P150 to P177 mice exposed to enriched conditions (Fig. 8). The typical tadpole morphology, firing pattern, and membrane properties (Marchionni et al. 2010; Quattrocolo and Maccaferri 2013) confirmed that labeled neurons were, as expected, Cajal–Retzius cells. The calculated membrane input resistance was 2.9 ± 0.3 and 2.7 ± 0.6 GΩ for the Wnt3a ($n = 12$) and for the PDE1c ($n = 5$) genotype, respectively ($P > 0.05$). In $n = 11$ cases where the anatomy of biocytin-filled cells was recovered, neurons were further confirmed to be Cajal–Retzius cells. Moreover, the pattern of reelin and calretinin immunolabeling of tdTomato-expressing cells yielded similar results to what obtained at earlier developmental stages (compare Figs 2 and 8 obtained in a P36 vs. P112 mouse).

Lastly, we decided to address the potential functional impact of this type of experience-dependent plasticity on the hippocampal network. Cajal–Retzius cells generate synaptic glutamatergic excitatory drive onto GABAergic interneurons of the molecular

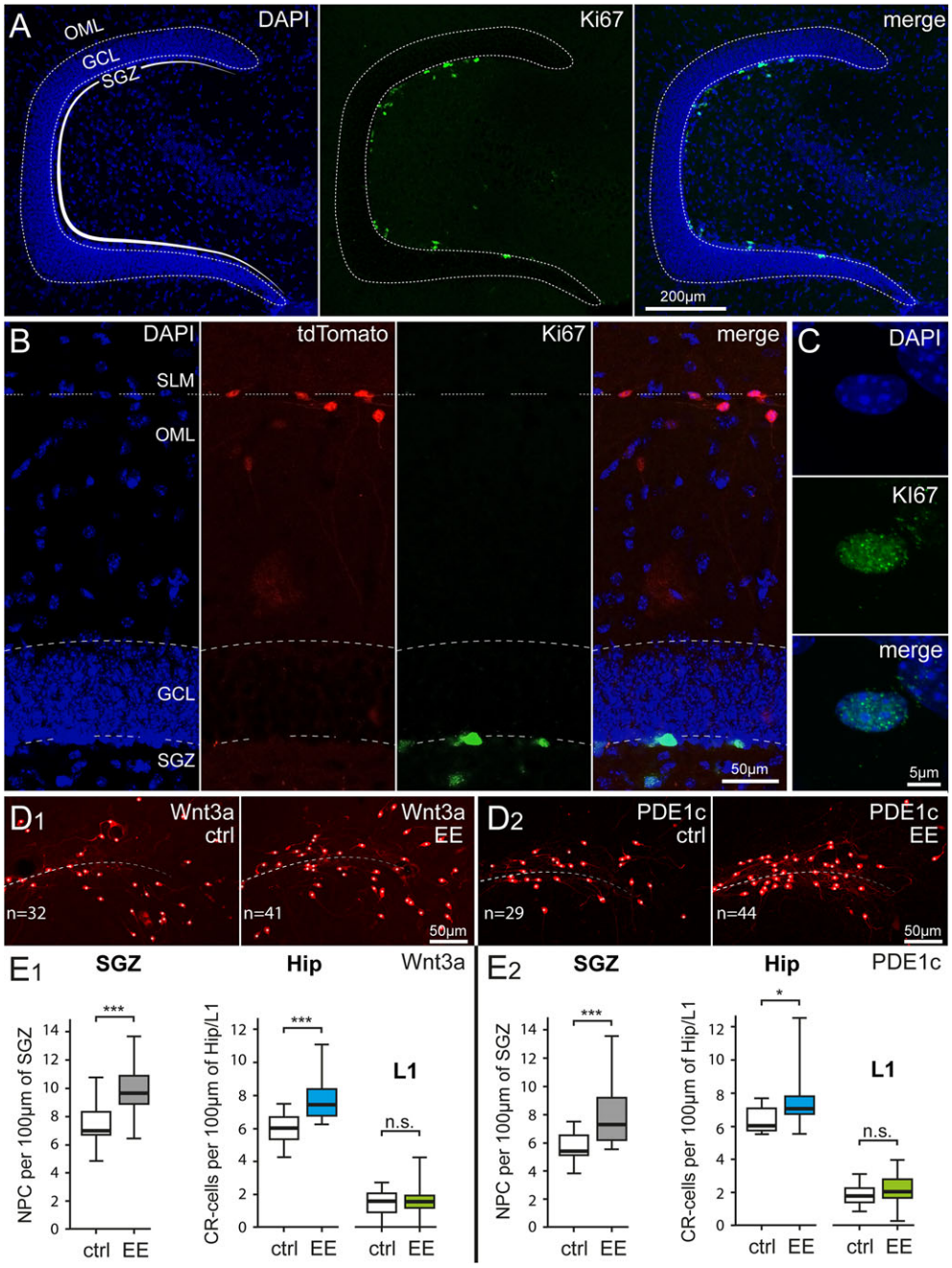

Figure 4. Parallel impact of enriched housing conditions on hippocampal neurogenesis and Cajal–Retzius cell density. (*A*) Identification of proliferating cells in the subgranular zone (SGZ) of the dentate gyrus by Ki-67 immunoreactivity. Left panel: DAPI counterstaining, middle panel: Ki-67-labeled nuclei, and right panel: previous images superimposed. OML, outer molecular layer; GCL, granule cell layer. (*B*) Simultaneous identification of dentate gyrus structure (left: DAPI counterstaining), Cajal–Retzius cells (middle left: tdTomato fluorescence), dividing cells (middle right: Ki67), and superimposition of all the images (right: merge). SLM, stratum lacunosum-moleculare. (*C*) High resolution image of a Ki-67-labeled nucleus in the SGZ. Top, middle, and bottom panels show DAPI counterstaining, Ki-67 immunoreactivity, and the 2 images overlapped, respectively. (*D1*) Comparison of Cajal–Retzius cell densities in a control Wnt3a mouse (ctrl) versus an animal housed in environmental enriched conditions (EE). Notice the increased numbers of Cajal–Retzius cells in the image from the treated mouse (n = 32 vs. 41, respectively). (*D2*) Same as in (*D1*), but for PDE1c animals. (*E1*) Summary plots showing the densities of Ki-67-positive nuclei of neural progenitor cells (NPC) (left panel) and of Cajal–Retzius cells (in the hippocampus: Hip and in layer 1 of the adjacent cortex: L1, right panel) of Wnt3a mice housed in control (ctrl) and environmental enriched (EE) conditions (left panel). (*E2*) Same analysis as in (*E1*) carried on in sections from PDE1c mice.

layers (Anstötz et al. 2016), which can be triggered by optogenetic stimulation (Quattrocolo and Maccaferri 2014). Therefore, increased densities of Cajal–Retzius cells in the hippocampus of mice exposed to enhanced environmental conditions would predict that optogenetic stimulation of Cajal–Retzius cells from these latter animals should also produce synaptic currents of larger amplitude onto interneurons. This expectation was directly tested by taking advantage of Wnt3a-ChR mice (for details see Materials and Methods and Quattrocolo and Maccaferri 2014), and confirmed by the results of Figure 9. A brief flash of blue light produced larger synaptic currents in interneurons from treated versus control animals (166 ± 41 pA, n = 21 vs.

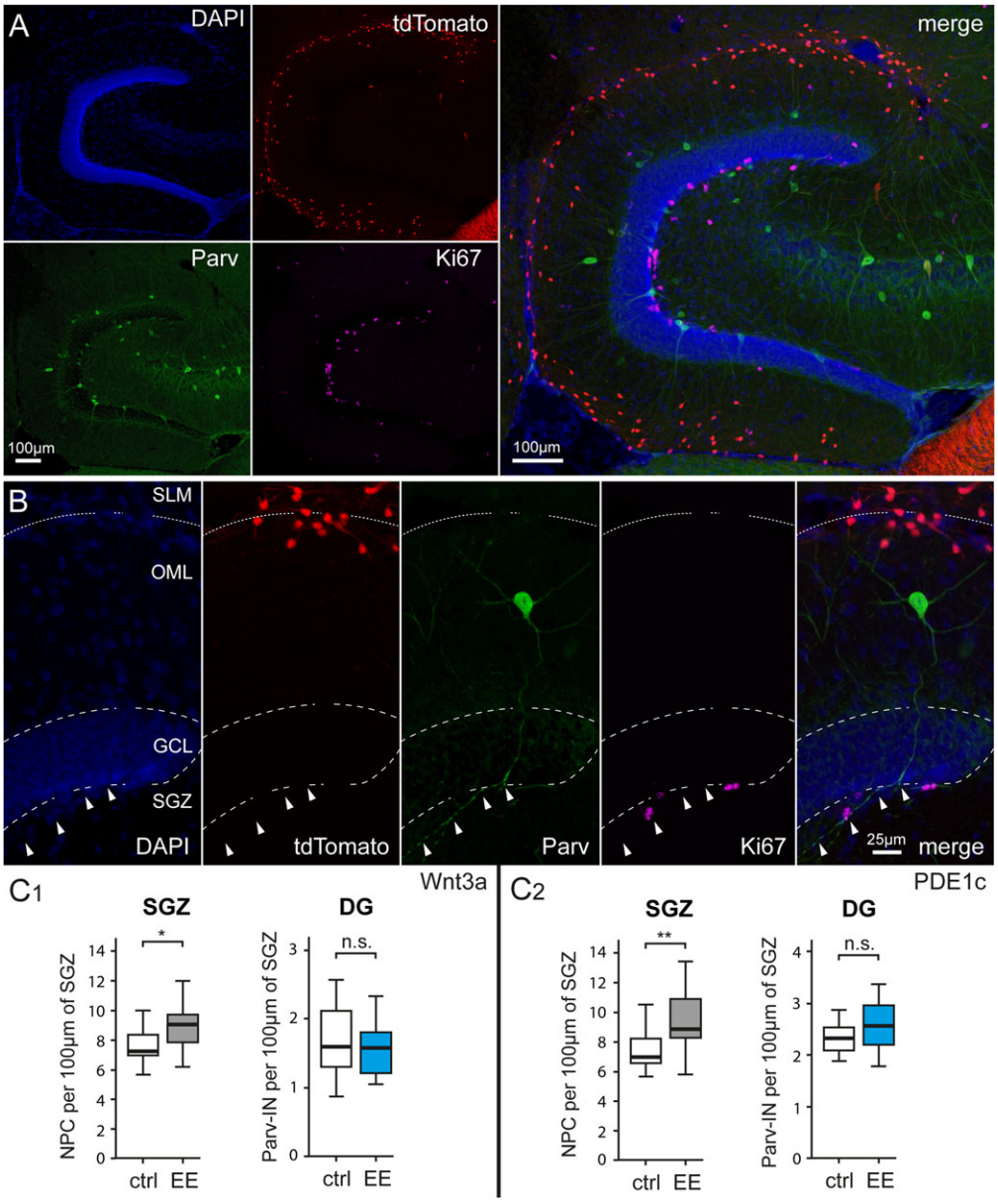

Figure 5. Environmental enrichment does not affect the densities parvalbumin-expressing interneurons of the dentate gyrus. (A) Identification of parvalbumin-expressing interneurons and proliferating cells in the denate gyrus of a P36 Wnt3a mouse. Top left panel: DAPI counterstaining, top middle panel: tdTomato-labeled cells, bottom left panel: parvalbumin immunohistochemistry, and middle right panel: Ki67 expression in the subgranular zone. The right panel shows all previous images superimposed. Please notice the much larger number of tdTomato expressing Cajal–Retzius cells compared with parvalbumin-labeled interneurons. (B) Left to right: identification at higher magnification of dentate gyrus structure (DAPI counterstaining), Cajal–Retzius cells (tdTomato fluorescence), parvalbumin-positive interneurons (Parv), dividing cells (Ki67), and superimposition of all the images (merge). Arrowheads indicate the main axonal trunk of the interneuron coasting the subgranular zone. (C1) Summary plots showing the densities of Ki-67-positive nuclei of neural progenitor cells (NPC) (left panel) and of parvalbumin immunoreactive cells in Wnt3a mice housed in control (ctrl) and environmental enriched (EE) conditions (left panel). Notice the selective effect of environmental enrichment on neural progenitors compared with interneurons. (C2) Same analysis as in (C1) carried out in sections from PDE1c mice.

96 ± 22 pA, n = 22, respectively, $P < 0.05$). No significant differences were found in the latency of the synaptic response (4.5 ± 0.3 ms and 4.7 ± 0.2 ms in treated vs. control animals, $P > 0.05$), consistent with the most parsimonious interpretation of a simple increase in Cajal–Retzius cell density in the absence of other functional changes. We also verified that the structural properties of the interneurons in the 2 groups (a total of n = 32 cells could be recovered) were comparable in layer distribution, dendritic length, and complexity. The total dendritic length was 1680.44 ± 189.04 µm, n = 16 versus 1627.54 ± 162.89 µm, n = 16, $P > 0.05$ in control versus treated animals, respectively, and no significant differences could be revealed by analyzing dendritic complexity by means of Sholl analysis (Fig. 9).

Discussion

The main results of this work are the unequivocal demonstrations that Cajal–Retzius cell networks persist at high densities in the fully mature hippocampus, and that they can be dynamically regulated by experience, in a region-specific manner.

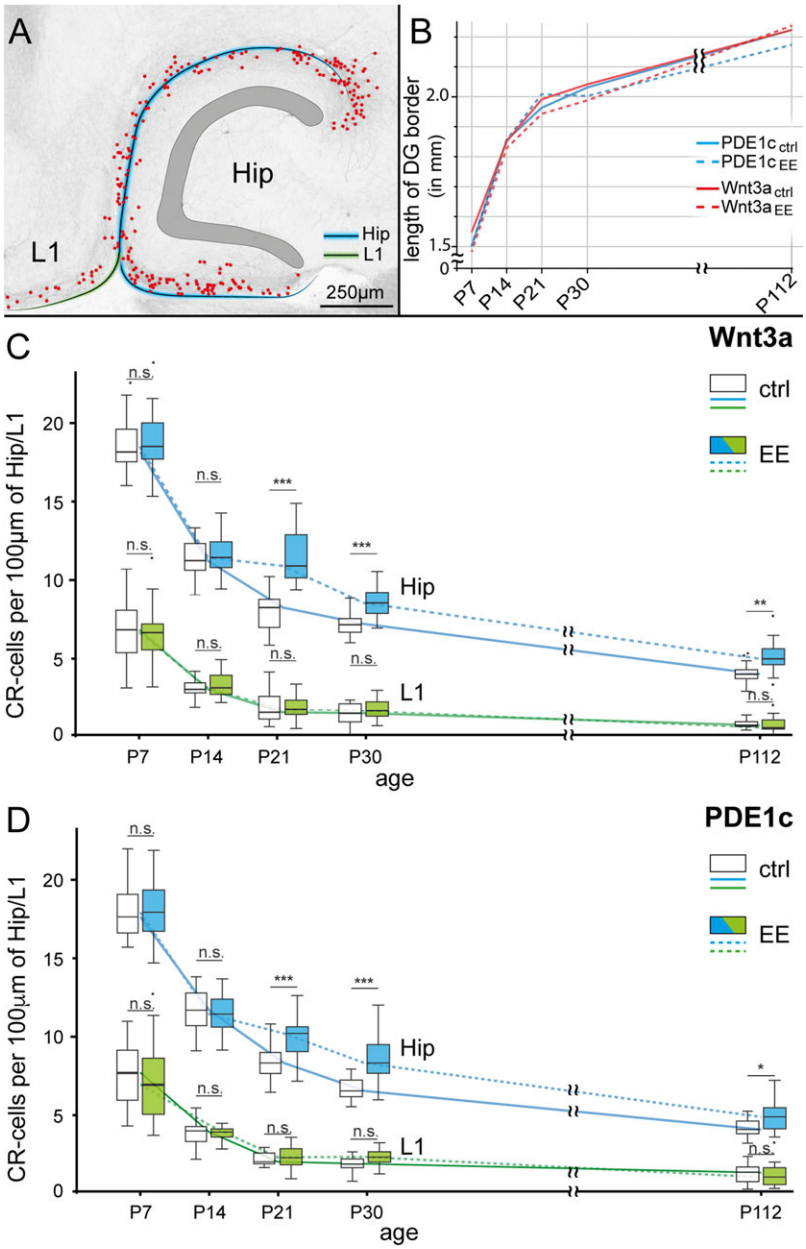

Figure 6. Region-specific developmental regulation and effect of enriched environment on Cajal–Retzius cells. (*A*) Sample image showing the 2 regions taken into consideration for the presented analysis: molecular layers of the hippocampus (along the hippocampal fissure and the infrapyramidal blade of the dentate gyrus: blue line) and layer 1 (L1) of the adjacent cortical areas (green line). CR-cell positions are marked by red dots. (*B*) Summary plot of the growth curve for the different mouse genotypes and experimental conditions (ctrl = control, EE = enriched environment) measured by the border-length of the dentate gyrus (see blue line in [A]). Notice the lack of any significant difference ($P > 0.05$). (*C*) Developmental time-course of hippocampal (blue lines) and layer 1 (green lines) Cajal–Retzius cell density under control (ctrl, solid line) and environmental enriched (EE, dotted lines) conditions. Box plots for different conditions at the same age have been shifted side by side to allow comparisons. Please notice the effect of EE on hippocampal, but not layer one Cajal–Retzius cells. Data from Wnt3a mice. (*D*) Same as in (*C*), but obtained in sections from PDE1c mice. Notice the similarity of the results in the 2 different reporter strains.

These findings suggest novel, experimentally testable, hypotheses regarding their potential involvement in the modulation of hippocampal adult neurogenesis.

Are Cajal–Retzius Cells an Integral Part of the Fully Mature Hippocampal Circuit?

Here, we show that Cajal–Retzius cells persist in the fully mature hippocampus at densities similar to what observed in adjacent cortical areas at much earlier postnatal stages. Compared with previous work, 3 important points make our current findings compelling. First, our interpretations are based on the converging results obtained using 2 different mouse strains. Second, Cre-loxP recombination avoids the potential problem of the developmental regulation of the chosen molecular marker/gene associated with immunohistochemistry and BAC transgenic mice. Third, we corroborated our results by filling labeled cells of the hippocampal molecular layers with

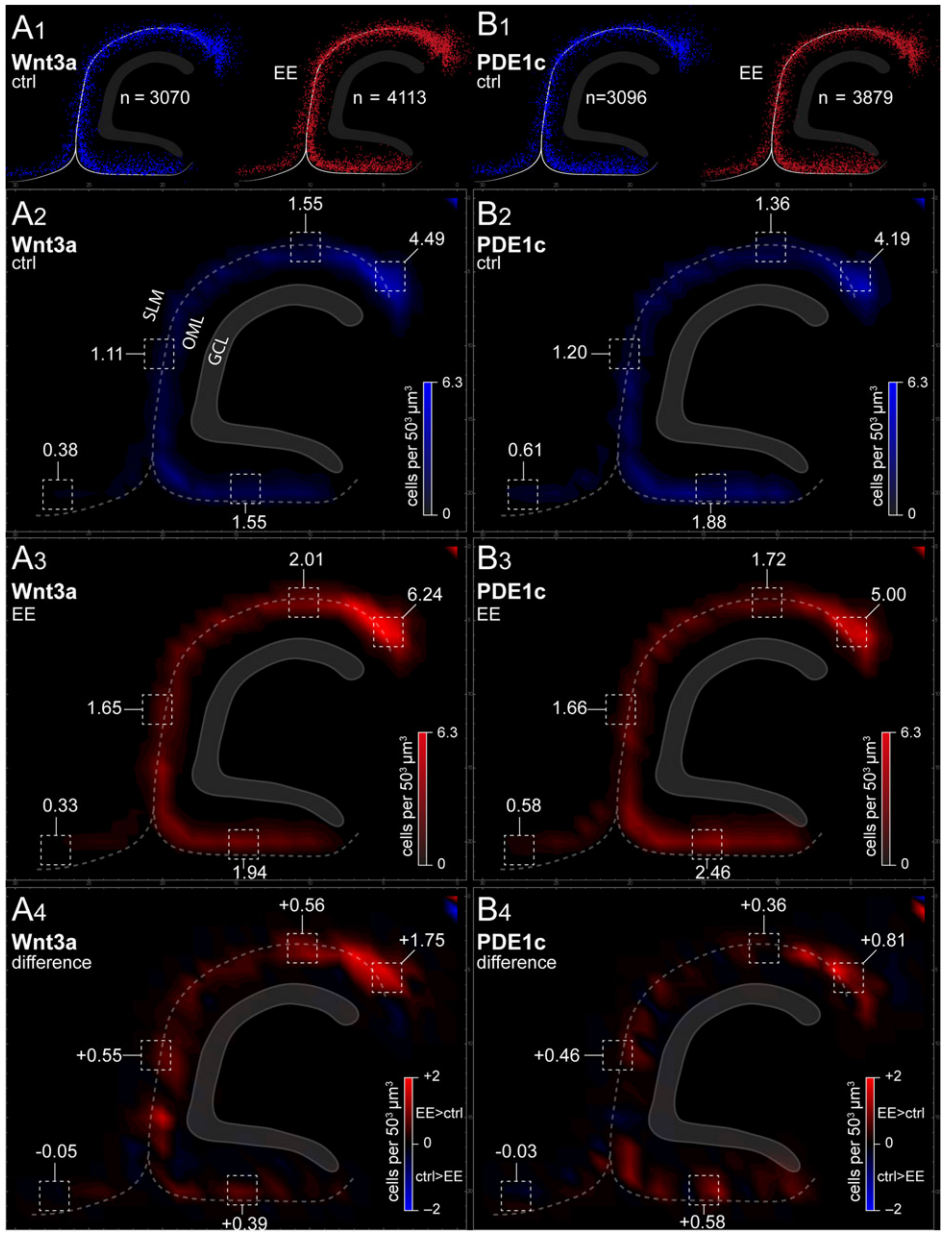

Figure 7. Summary plots of Cajal–Retzius cell distributions along the hippocampal molecular layers and cortical layer 1. (A1) Raw dot plots indicating the distribution of all Cajal–Retzius cells analyzed (P21 Wnt3a mouse). Left panel: control group (ctrl, blue dots). Right panel: environmental enriched conditions (EE, red dots). Notice the higher numbers of Cajal–Retzius cells in the latter group. (A2,A3) Summary density graphs for animals housed in control (blue scale) and enriched conditions (red scale). (A4) Plot of the overall density difference between the 2 experimental conditions. Notice the increased density distributed broadly along the hippocampal molecular fields, but the lack of change in layer 1 of the adjacent cortex. (B1–B4) As in (A1–A4), but for PDE1c animals.

biocytin and by recording their electrophysiological properties. We always found the typical morphology and functional signatures of Cajal–Retzius cells. In fact, this work also provides, for the first time, direct recordings from Cajal–Retzius cell of slices from fully mature animals (P150–P177).

Thus, our data radically change past views of Cajal–Retzius cells as a transient neuronal type, exclusively associated with developmental functions, and show that their disappearance or persistence depends on the specific cortical area considered. How could this region-specificity arise? Cajal–Retzius cells are produced by different sites during development (Bielle et al. 2005) and reach specific cortical domains (Griveau et al. 2010) by tangential migration regulated by contact repulsion (Villar-Cerviño et al. 2013). Therefore, the region-specific densities of Cajal–Retzius cells could be either explained by their ontogenetic origin, by local environmental signaling factors or by both factors combined. While we are not aware of any ontogentic specificity in the expression of PDE1c, Wnt3a is an accepted marker of hem-derived Cajal–Retzius cells (Louvi et al. 2007). Therefore, our finding of a differential regulation of hippocampal versus cortical Cajal–Retzius cells of the Wnt3a lineage rules out the ontogenetic origin as a unique satisfactory explanation (see Ledonne et al. 2016 for the impact of the ontogenetic origin in molecular mechanisms leading to Cajal–Retzius cell death), and points to the potential importance of local survival/death factors, and, possibly, specific patterns of

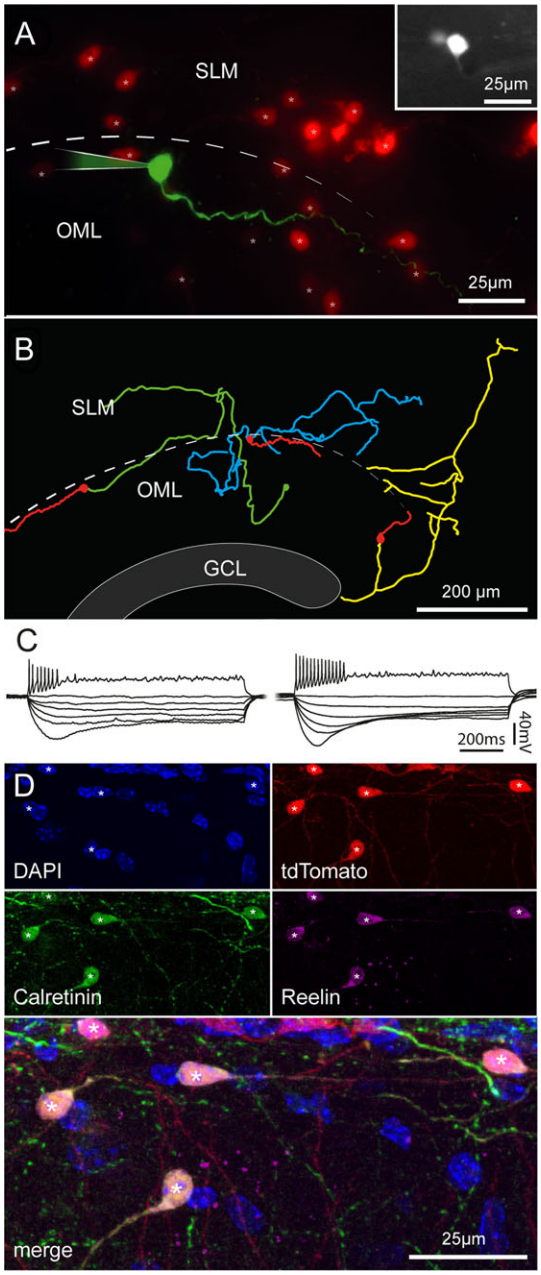

Figure 8. Morphofunctional properties and immunoreactivity of Cajal–Retzius cells in fully mature mice. (*A*) Pseudocolor image of a biocytin-filled cell (green) form a P153 Wnt3a animal housed under enriched conditions. Other tdTomato-labeled cells are shown in red. Notice the typical tadpole morphology. Inset at the top right shows a fluorescent image of the same cell in the living slice. SLM, stratum lacunosum-moleculare; OML, outer molecular layer, dotted line: hippocampal fissure. (*B*) Morphological reconstruction of 3 Cajal–Retzius cells from adult mice (Wnt3a, enriched conditions from left to right: P153, P150, and P150). Notice the typical distribution pattern of dendrites and axons. Dendrites: red, axons: green, blue, and yellow. GCL, granule cell layer. (*C*) Firing patterns and membrane properties recorded in Cajal–Retzius cells of adult mice (P150–P177). Notice the similarity with what recorded in younger animals shown in Figure 2. (*D*) Cajal–Retzius cells from mature animals express calretinin and reelin. Images from a P112 Wnt3a mouse (housed in control conditions) showing DAPI nuclear counterstaining and labeling of tdTomato, calretinin, and reelin in single pictures, and superimposed. Notice the typical tadpole-like morphology of the cells identified by asterisks. Compare to Figure 2.

neuronal activity (as suggested by work performed in organotypic cultures: Del Río et al. 1996; Blanquie et al. 2016).

Cellular and Synaptic Functions of Cajal–Retzius Cells in the Postnatal Hippocampus

A lot of attention and experimental efforts have been directed toward understanding the roles of Cajal–Retzius cells at early developmental stages, highlighting the fact that they are a cellular source of the glycoprotein reelin. In the hippocampus, reelin has been shown to be important for the correct development of layer-specific connections (Del Río et al. 1997; Borrell et al. 1999) and for the formation of the radial glia scaffold that leads to the correct positioning of neurons (Förster et al. 2002). Furthermore, reelin appears to be involved in additional functions in the mature hippocampus, such as the correct maintenance of adult neurogenesis (Zhao et al. 2007; Pujadas et al. 2010; Teixeira et al. 2012), synaptic function/plasticity (Weeber et al. 2002; Qiu et al. 2006; Pujadas et al. 2010; Ventruti et al. 2011), prevention of granule cell dispersion (Heinrich et al. 2006; Duveau et al. 2011; Tinnes et al. 2011), and preservation of the architectural integrity of the CA1 region (Jiang et al. 2016). However, reelin expression by Cajal–Retzius cells has been reported to undergo down-regulation with brain maturation (Ringstedt et al. 1998). Furthermore, Cajal–Retzius cells are not the unique cellular source of reelin in the mature brain, as this role is also played by GABAergic interneurons (Pesold et al. 1998), such as neurogliaform cells (Fuentealba et al. 2010, for a review on neurogliaform cells, see: Armstrong et al. 2012).

Therefore, in addition to potential reelin-dependent roles, the persistence of Cajal–Retzius cells in the postnatal hippocampus might be linked to specific effects exerted on their postsynaptic target neurons. In fact, Cajal–Retzius cells provide strong excitatory input to interneurons (Anstötz et al. 2016), potentially resulting in the feed-forward activation of neurogliaform cells (Quattrocolo and Maccaferri 2014), and/or other interneurons which are a critical source of GABAergic input for newborn granule cells (Markwardt et al. 2011, Waterhouse et al. 2012; Song et al. 2013).

Effect of Environmental Enrichment on Cajal–Retzius Cell Densities: Potential Mechanisms

Our work unveils for the first time that the density of Cajal–Retzius cell in the hippocampus can be modulated by behavioral manipulations. In particular, we used experimental protocols that are commonly associated with enhanced postnatal neurogenesis (Kempermann et al. 1997) because of the striking parallels between the unique permanence of Cajal–Retzius cells in the adult hippocampus compared with other cortical areas and the uniqueness of the hippocampus as an adult neurogenic cortical region. It is also intriguing to note that the decline of Cajal–Retzius cell density shown here has a roughly similar time-course to the decrease in mouse postnatal neurogenesis reported by several papers (Ben Abdallah et al. 2010; Raman et al. 2011; Ansorg et al. 2012; Oishi et al. 2016).

Our experimental conditions were complex because enrichment included both supplemental nesting material (promoting more physiological behaviors) and running (spinning wheel). Running, in particular, has been reported to strongly impact cell

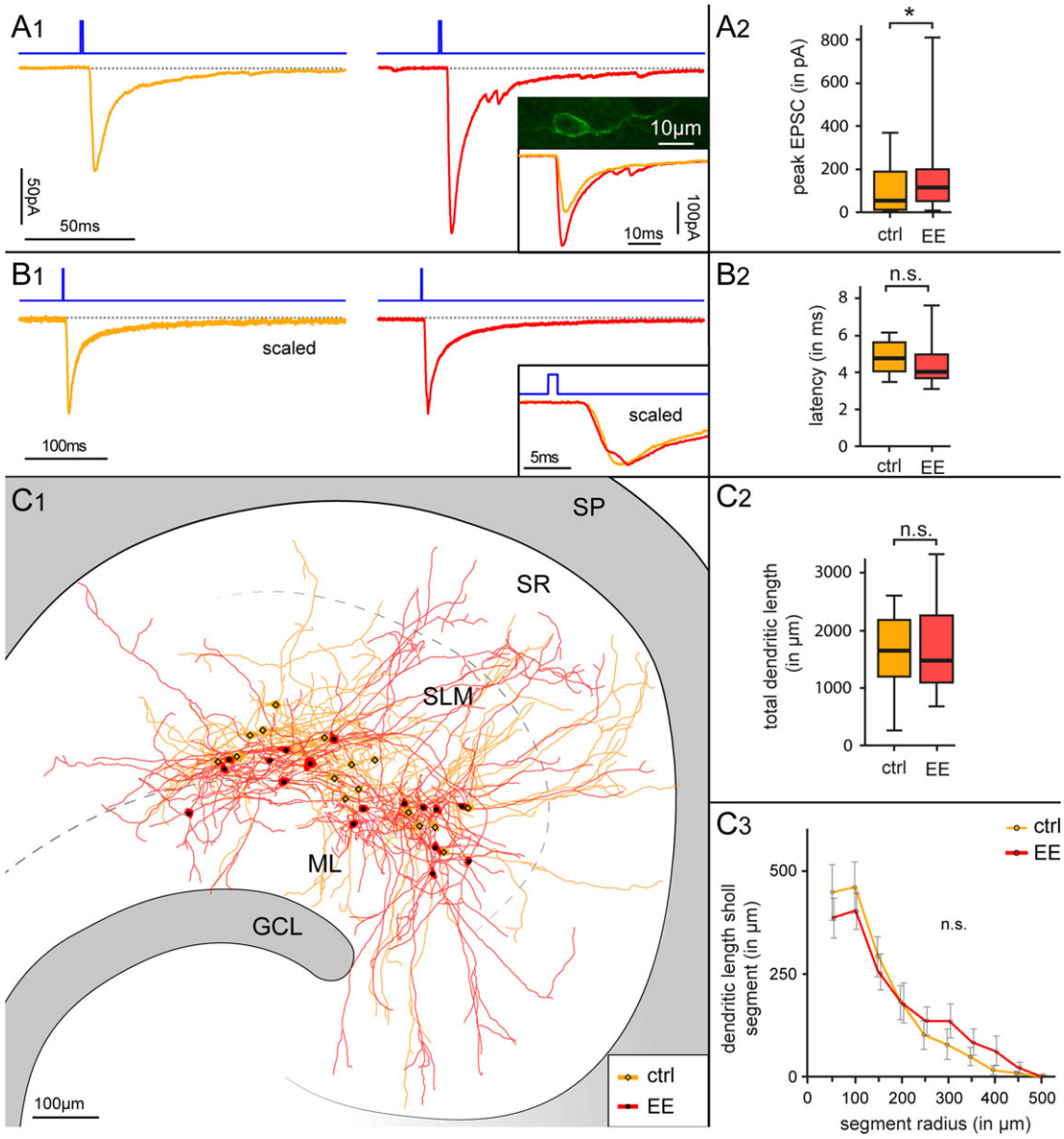

Figure 9. Functional impact of environmental enriched conditions on synaptic currents generated by Cajal–Retzius cells onto interneurons. (A1) Optogenetic stimulation of Cajal–Retzius cells in slices obtained from Wnt3a-ChR mice housed in standard versus enriched conditions. Notice the larger synaptic current evoked in interneurons in the treated (right, red trace) when compared with the control group (left, dark yellow trace). Duration of light flash stimulation (1 ms) is indicated by the blue line above the recordings. The inset shows the eYFP confocal image of a typical Cajal–Retzius cell in the Wnt3a-ChR mouse. (A2) Summary box chart comparing the peak amplitude of the optogenetically evoked EPSCs in control (ctrl) versus animals exposed to environmental enrichment (EE). (B1) Optogenetically evoked EPSCs in interneurons recorded from slices obtained from control versus treated animals have similar kinetic properties and latencies. Averaged scaled traces of all the recordings in control mice (dark yellow trace, left) and in animals exposed to enriched conditions (red trace, right). Traces are superimposed in the bottom right inset: notice the similar kinetics and latency. (B2) Population plot for EPSC latencies measured in the 2 groups of animals. (C1–C3) Similar location and dendritic properties of postsynaptic interneurons receiving Cajal–Retzius cell-generated synaptic input suggests that the different amplitude of optogenetic responses does not depend on postsynaptic differences. (C1) NEUROLUCIDA reconstruction of 32 interneurons in slices from control (ctrl, $n = 16$, dark yellow) vand treated mice (EE, $n = 16$, red). Notice the similar localization along the hippocampal fissure. GCL, granule cell layer; ML, molecular layer; SLM, stratum lacunosum-moleculare; SR, stratum radiatum; SP, stratum pyramidale. (C2) Quantitative analysis of the dendritic length measured in the reconstructed cells does not reveal significant differences between control (ctrl) versus treated (EE) groups. (C3) Dendritic complexity evaluated by Sholl analysis for mice housed under standard (ctrl) and enriched conditions (EE). Notice the lack of significant differences.

proliferation of neural progenitor cells, whereas a variety of different enrichments (not immediately associated with motor activity) are believed to regulate the survival of neurons at critical stages of maturation (van Praag et al. 1999, see also review by Aimone et al. 2014). Furthermore, running has been shown to be the critical neurotrophic stimulus of enriched conditions that trigger increased levels of hippocampal BDNF (Kobilo et al. 2011).

Although Cajal–Retzius cells express TrKB receptors since early stages (Fukumitsu et al. 1998), the functions of this signaling may change during brain maturation. In fact, during early development, BDNF-TrkB signaling is believed to be important in setting the physiological spatial organization of Cajal–Retzius cells, which then orchestrates the correct development of cortical networks (Alcántara et al. 2006). Furthermore,

although BDNF does not appear to be required for Cajal–Retzius cell survival at early postnatal stages (<P11), reelin-expressing cells of the marginal zone were reported at lower numbers in BDNF−/− mice at later times (Ringstedt et al. 1998). In addition, increased TrkB signaling was proposed to mediate the increased survival of neocortical Cajal–Retzius cells of developing mice exposed to cortical freezing lesions (Supèr et al. 1997). All the aforementioned considerations suggest the equally intriguing and potentially simple mechanistic scenario where increased BDNF levels produced by running (Kobilo et al. 2011) promote Cajal–Retzius cell survival and result in the higher densities observed in our experimental groups. It is also important to note that BNDF effects on the maturation of newborn granule cells are mediated by enhancing GABA release (Waterhouse et al. 2012), which could depend, in part, by stronger excitation of interneurons due to increased Cajal–Retzius cell densities.

Although our present data reveal similarities in the developmental time-course and impact of environmental conditions on Cajal–Retzius cells and neurogenesis, establishing a detailed mechanistic link will require further work. Furthermore, it needs to be acknowledged that environmental enrichment is a very powerful stimulus that produces many complex changes in the brain at various levels (van Praag et al. 2000). Therefore, our finding of an apparent correlation between experience-dependent modulation of Cajal–Retzius cell densities and neurogenesis may not reflect either a causal link or a functional relationship as we speculate. For example, increased Cajal–Retzius cells glutamatergic input onto GABAergic interneurons may be part of the chain of events that links exposure to enriched environment to a beneficial effect observed in experimental animal models of epilepsy (reviewed by Kotloski and Sutula 2015). The relationship between increased density of Cajal–Retzius cells and neurogenesis will be clarified by future experiments targeting this process with anti-mitotic treatments, irradiation, and/or by the study of animal models with genetic deletion of either neuronal progenitor cells (Deng et al. 2010) or Cajal–Retzius cells (Tissir et al. 2009).

Conclusions

In summary, our data unequivocally show that hippocampal Cajal–Retzius cells remain in the fully mature hippocampus and that their densities can be modulated by experience using protocols that also affect hippocampal postnatal neurogenesis. We propose that Cajal–Retzius cells may play a functional role in the regulation of the hippocampal neurogenic niche.

Funding

National Institutes of Health (grant NS064135 and supplement NS064135S1 to G.M.).

Notes

We would like to thank Dr Marco Martina for helpful comments and critical reading of the manuscript. We are also grateful to Dr Antonio Virgilio Failla and to the University Medical Center Hamburg-Eppendorf Microscopy Imaging for technical support and help with confocal microscopes. *Conflict of Interest*: None declared.

References

Abraham H, Meyer G. 2003. Reelin-expressing neurons in the postnatal and adult human hippocampal formation. Hippocampus. 13:715–727.

Abraham H, Toth Z, Seress L. 2004. A novel population of calretinin positive neurons comprises reelin-positive Cajal-Retzius cells in the hippocampal formation of the adult domestic pig. Hippocampus. 14:385–401.

Aimone JB, Li Y, Lee SW, Clemenson GD, Deng W, Gage FH. 2014. Regulation and function of adult neurogenesis: from genes to cognition. Physiol Rev. 94:991–1026.

Alcántara S, Pozas E, Ibañez CF, Soriano E. 2006. BDNF-modulated spatial organization of Cajal-Retzius and GABAergic neurons in the marginal zone plays a role in the development of cortical organization. Cereb Cortex. 16:487–499.

Ansorg A, Witte OW, Urbach A. 2012. Age-dependent kinetics of dentate gyrus neurogenesis in the absence of cyclin D2. BMC Neurosci. 13:46.

Anstötz M, Cosgrove KE, Hack I, Mugnaini E, Maccaferri G, Lübke JH. 2014. Morphology, input-output relations and synaptic connectivity of Cajal-Retzius cells in layer 1 of the developing neocortex of CXCR4-EGFP mice. Brain Struct Funct. 219:2119–2139.

Anstötz M, Huang H, Marchionni I, Haumann I, Maccaferri G, Lübke JH. 2016. Developmental profile, morphology, and synaptic connectivity of Cajal-Retzius cells in the postnatal mouse hippocampus. Cereb Cortex. 26:855–872.

Armstrong C, Krook-Magnuson E, Soltesz I. 2012. Neurogliaform and Ivy cells: a major family of nNOS expressing GABAergic neurons. Front Neural Circuits. 16:6–23.

Bagri A, Gurney T, He X, Zou YR, Littman DR, Tessier-Lavigne M, Pleasure SJ. 2002. The chemokine SDF1 regulates migration of dentate granule cells. Development. 129: 4249–4260.

Ben Abdallah NMB, Slomianka L, Vyssotski AL, Lipp HP. 2010. Early age-related changes in adult hippocampal neurogenesis in C57 mice. Neurobiol Aging. 31:151–161.

Bielle F, Griveau A, Narboux-Nême N, Vigneau S, Sigrist M, Arber S, Wassef M, Pierani A. 2005. Multiple origins of Cajal-Retzius cells at the borders of the developing pallium. Nat Neurosci. 8:1002–1012.

Blanquie O, Liebmann L, Hübner CA, Luhmann HJ, Sinning A. 2016. NKCC1-mediated GABAergic signaling promotes postnatal cell death in neocortical Cajal-Retzius cells. Cereb Cortex. 2016 Jan 27. pii:bhw004. [Epub ahead of print]

Blasco-Ibáñez JM, Freund TF. 1997. Distribution, ultrastructure, and connectivity of calretinin-immunoreactive mossy cells of the mouse dentate gyrus. Hippocampus. 7:307–320.

Borrell V, Del Río JA, Alcántara S, Derer M, Martínez A, D'Arcangelo G, Nakajima K, Mikoshiba K, Derer P, Curran T, et al. 1999. Reelin regulates the development and synaptogenesis of the layer-specific entorhino-hippocampal connections. J Neurosci. 19:1345–1358.

Chowdhury TG, Jimenez JC, Bomar JM, Cruz-Martin A, Cantle JP, Portera-Cailliau C. 2010. Fate of cajal-retzius neurons in the postnatal mouse neocortex. Front Neuroanat. 4:10.

Coppola E, Ledonné F, Pierani A. 2015. Subtype specific persistence of Cajal-Retzius cells in the postnatal mouse brain. Int J Dev Neurosci. 47:23–24.

Del Río JA, Heimrich B, Borrell V, Förster E, Drakew A, Alcántara S, Nakajima K, Miyata T, Ogawa M, Mikoshiba K, et al. 1997. A role for Cajal-Retzius cells and reelin in the development of hippocampal connections. Nature. 385:70–74.

Del Río JA, Heimrich B, Supèr H, Borrell V, Frotscher M, Soriano E. 1996. Differential survival of Cajal-Retzius cells in organotypic cultures of hippocampus and neocortex. J Neurosci. 16:6896–6907.

del Rio JA, Martinez A, Fonseca M, Auladell C, Soriano E. 1995. Glutamate-like immunoreactivity and fate of Cajal-Retzius cells in the murine cortex as identified with calretinin antibody. Cereb Cortex. 5:13–21.

Deng W, Aimone JB, Gage FH. 2010. New neurons and new memories: how does adult hippocampal neurogenesis affect learning and memory? Nat Rev Neurosci. 11:339–350.

Derer P, Derer M. 1990. Cajal–Retzius cell ontogenesis and death in mouse brain visualized with horseradish peroxidase and electron microscopy. Neuroscience. 36:839–856.

Duveau V, Madhusudan A, Caleo M, Knuesel I, Fritschy JM. 2011. Impaired reelin processing and secretion by Cajal-Retzius cells contributes to granule cell dispersion in a mouse model of temporal lobe epilepsy. Hippocampus. 21:935–944.

Förster E, Tielsch A, Saum B, Weiss KH, Johanssen C, Graus-Porta D, Müller U, Frotscher M. 2002. Reelin, disabled 1, and beta 1 integrins are required for the formation of the radial glial scaffold in the hippocampus. Proc Natl Acad Sci USA. 99:13178–13183.

Frotscher M. 1998. Cajal-Retzius cells, reelin, and the formation of layers. Curr Opin Neurobiol. 8:570–575.

Fuentealba P, Klausberger T, Karayannis T, Suen WY, Huck J, Tomioka R, Rockland K, Capogna M, Studer M, Morales M, et al. 2010. Expression of COUP-TFII nuclear receptor in restricted GABAergic neuronal populations in the adult rat hippocampus. J Neurosci. 30:1595–1609.

Fukumitsu H, Furukawa Y, Tsusaka M, Kinukawa H, Nitta A, Nomoto H, Mima T, Furukawa S. 1998. Simultaneous expression of brain-derived neurotrophic factor and neurotrophin-3 in Cajal-Retzius, subplate and ventricular progenitor cells during early development stages of the rat cerebral cortex. Neuroscience. 84:115–127.

Gil V, Nocentini S, Del Río JA. 2014. Historical first descriptions of Cajal-Retzius cells: from pioneer studies to current knowledge. Front Neuroanat. 8:32.

Gil-Sanz C, Franco SJ, Martinez-Garay I, Espinosa A, Harkins-Perry S, Müller U. 2013. Cajal-Retzius cells instruct neuronal migration by coincidence signaling between secreted and contact-dependent guidance cues. Neuron. 79:461–477.

Griveau A, Borello U, Causeret F, Tissir F, Boggetto N, Karaz S, Pierani A. 2010. A novel role for Dbx1-derived Cajal-Retzius cells in early regionalization of the cerebral cortical neuroepithelium. PLoS Biol. 8:e1000440.

Gu X, Liu B, Wu X, Yan Y, Zhang Y, Wei Y, Pleasure SJ, Zhao C. 2011. Inducible genetic lineage tracing of cortical hem derived Cajal-Retzius cells reveals novel properties. PLoS One. 6:e28653.

Gulyás AI, Hájos N, Freund TF. 1996. Interneurons containing calretinin are specialized to control other interneurons in the rat hippocampus. J Neurosci. 16:3397–3411.

Heinrich C, Nitta N, Flubacher A, Müller M, Fahrner A, Kirsch M, Freiman T, Suzuki F, Depaulis A, Frotscher M, et al. 2006. Reelin deficiency and displacement of mature neurons, but not neurogenesis, underlie the formation of granule cell dispersion in the epileptic hippocampus. J Neurosci. 26:4701–4713.

Jiang Y, Gavrilovici C, Chansard M, Liu RH, Kiroski I, Parsons K, Park SK, Teskey GC, Rho JM, Nguyen MD. 2016. Ndel1 and reelin maintain postnatal CA1 hippocampus integrity. J Neurosci. 36:6538–6552.

Kee N, Sivalingam S, Boonstra R, Wojtowicz JM. 2002. The utility of Ki-67 and BrdU as proliferative markers of adult neurogenesis. J Neurosci Methods. 115:97–105.

Kempermann G, Kuhn HG, Gage FH. 1997. More hippocampal neurons in adult mice living in an enriched environment. Nature. 386:493–495.

Kobilo T, Liu QR, Gandhi K, Mughal M, Shaham Y, van Praag H. 2011. Running is the neurogenic and neurotrophic stimulus in environmental enrichment. Learn Mem. 18:605–609.

Kolodziej A, Schulz S, Guyon A, Wu DF, Pfeiffer M, Odemis V, Höllt V, Stumm R. 2008. Tonic activation of CXC chemokine receptor 4 in immature granule cells supports neurogenesis in the adult dentate gyrus. J Neurosci. 28:4488–4500.

Kotloski RJ, Sutula TP. 2015. Environmental enrichment: evidence for an unexpected therapeutic influence. Exp Neurol. 264:121–126.

Ledonne F, Orduz D, Mercier J, Vigier L, Grove EA, Tissir F, Angulo MC, Pierani A, Coppola E. 2016. Targeted inactivation of bax reveals a subtype-specific mechanism of Cajal-Retzius neuron death in the postnatal cerebral cortex. Cell Rep. 17:3133–3141.

Louvi A, Yoshida M, Grove EA. 2007. The derivatives of the Wnt3a lineage in the central nervous system. J Comp Neurol. 504:550–569.

Madisen L, Mao T, Koch H, Zhuo JM, Berenyi A, Fujisawa S, Hsu YW, Garcia AJ3rd, Gu X, Zanella S, et al. 2012. A toolbox of Cre-dependent optogenetic transgenic mice for light-induced activation and silencing. Nat Neurosci. 15: 793–802.

Marchionni I, Beaumont M, Maccaferri G. 2012. The chemokine CXCL12 and the HIV-1 envelope protein gp120 regulate spontaneous activity of Cajal-Retzius cells in opposite directions. J Physiol. 590:3185–3202.

Marchionni I, Takács VT, Nunzi MG, Mugnaini E, Miller RJ, Maccaferri G. 2010. Distinctive properties of CXC chemokine receptor 4-expressing Cajal-Retzius cells versus GABAergic interneurons of the postnatal hippocampus. J Physiol. 588: 2859–2878.

Marin-Padilla M. 1990. Three-dimensional structural organization of layer I of the human cerebral cortex: a Golgi study. J Comp Neurol. 299:89–105.

Markwardt SJ, Dieni CV, Wadiche JI, Overstreet-Wadiche L. 2011. Ivy/neurogliaform interneurons coordinate activity in the neurogenic niche. Nat Neurosci. 14:1407–1409.

Motulsky H. 2010. Intuitive biostatistics. Oxford (UK): Oxford University Press.

Nagy A. 2000. Cre recombinase: the universal reagent for genome tailoring. Genesis. 26:99–109.

Naqui SZ, Harris BS, Thomaidou D, Parnavelas JG. 1999. The noradrenergic system influences the fate of Cajal-Retzius cells in the developing cerebral cortex. Brain Res Dev Brain Res. 113:75–82.

Oishi S, Premarathne S, Harvey TJ, Iyer S, Dixon C, Alexander S, Burne TH, Wood SA, Piper M. 2016. Usp9x-deficiency disrupts the morphological development of the postnatal hippocampal dentate gyrus. Sci Rep. 6:25783.

Oppenheim RW, Flavell RA, Vinsant S, Prevette D, Kuan CY, Rakic P. 2001. Programmed cell death of developing mammalian neurons after genetic deletion of caspases. J Neurosci. 21:4752–4760.

Osheroff H, Hatten ME. 2009. Gene expression profiling of preplate neurons destined for the subplate: genes involved in transcription, axon extension, neurotransmitter regulation,

steroid hormone signaling, and neuronal survival. Cereb Cortex. 19:i126–i134.
Overstreet-Wadiche L, McBain CJ. 2015. Neurogliaform cells in cortical circuits. Nat Rev Neurosci. 16:458–468.
Parnavelas JG, Edmunds SM. 1983. Further evidence that Retzius–Cajal cells transform to nonpyramidal neurons in the developing rat visual cortex. J Neurocytol. 12:863–871.
Pesold C, Impagnatiello F, Pisu MG, Uzunov DP, Costa E, Guidotti A, Caruncho HJ. 1998. Reelin is preferentially expressed in neurons synthesizing gamma-aminobutyric acid in cortex and hippocampus of adult rats. Proc Natl Acad Sci USA. 95:3221–3226.
Pujadas L, Gruart A, Bosch C, Delgado L, Teixeira CM, Rossi D, de Lecea L, Martínez A, Delgado-García JM, Soriano E. 2010. Reelin regulates postnatal neurogenesis and enhances spine hypertrophy and long-term potentiation. J Neurosci. 30: 4636–4649.
Qiu S, Zhao LF, Korwek KM, Weeber EJ. 2006. Differential reelin-induced enhancement of NMDA and AMPA receptor activity in the adult hippocampus. J Neurosci. 26:12943–12955.
Quattrocolo G, Maccaferri G. 2013. Novel GABAergic circuits mediating excitation/inhibition of Cajal-Retzius cells in the developing hippocampus. J Neurosci. 33:5486–5498.
Quattrocolo G, Maccaferri G. 2014. Optogenetic activation of Cajal-Retzius cells reveals their glutamatergic output and a novel feedforward circuit in the developing mouse hippocampus. J Neurosci. 34:13018–13032.
Raman L, Kong X, Gilley JA, Kernie SG. 2011. Chronic hypoxia impairs murine hippocampal development and depletes the postnatal progenitor pool by attenuating mammalian target of rapamycin signaling. Pediatr Res. 70:159–175.
Ringstedt T, Linnarsson S, Wagner J, Lendahl U, Kokaia Z, Arenas E, Ernfors P, Ibáñez CF. 1998. BDNF regulates reelin expression and Cajal-Retzius cell development in the cerebral cortex. Neuron. 21:305–315.
Sarnat HB, Flores-Sarnat L. 2002. Role of Cajal–Retzius and subplate neurons in cerebral cortical development. Semin Pediatr Neurol. 9:302–308.
Saville DJ. 1990. Multiple comparison procedures: the practical solution. Am Stat. 44:174–180.
Song J, Sun J, Moss J, Wen Z, Sun GJ, Hsu D, Zhong C, Davoudi H, Christian KM, Toni N, et al. 2013. Parvalbumin interneurons mediate neuronal circuitry-neurogenesis coupling in the adult hippocampus. Nat Neurosci. 16:1728–1730.
Supèr H, Martínez A, Del Río JA, Soriano E. 1998. Involvement of distinct pioneer neurons in the formation of layer-specific connections in the hippocampus. J Neurosci. 18:4616–4626.
Supèr H, Pérez Sust P, Soriano E. 1997. Survival of Cajal-Retzius cells after cortical lesions in newborn mice: a possible role for Cajal-Retzius cells in brain repair. Brain Res Dev Brain Res. 98:9–14.
Teixeira CM, Kron MM, Masachs N, Zhang H, Lagace DC, Martinez A, Reillo I, Duan X, Bosch C, Pujadas L, et al. 2012. Cell-autonomous inactivation of the reelin pathway impairs adult neurogenesis in the hippocampus. J Neurosci. 32: 12051–12065.
Tinnes S, Schäfer MK, Flubacher A, Münzner G, Frotscher M, Haas CA. 2011. Epileptiform activity interferes with proteolytic processing of reelin required for dentate granule cell positioning. FASEB J. 25:1002–1013.
Tissir F, Ravni A, Achouri Y, Riethmacher D, Meyer G, Goffinet AM. 2009. DeltaNp73 regulates neuronal survival in vivo. Proc Natl Acad Sci USA. 106:16871–16876.
Tozuka Y, Fukuda S, Namba T, Seki T, Hisatsune T. 2005. GABAergic excitation promotes neuronal differentiation in adult hippocampal progenitor cells. Neuron. 47:803–815.
van Praag H, Kempermann G, Gage FH. 1999. Running increases cell proliferation and neurogenesis in the adult mouse dentate gyrus. Nat Neurosci. 2:84–90.
van Praag H, Kempermann G, Gage FH. 2000. Neural consequences of environmental enrichment. Nat Rev Neurosci. 1: 191–198.
Ventruti A, Kazdoba TM, Niu S, D'Arcangelo G. 2011. Reelin deficiency causes specific defects in the molecular composition of the synapses in the adult brain. Neuroscience. 189:32–42.
Villar-Cerviño V, Molano-Mazón M, Catchpole T, Valdeolmillos M, Henkemeyer M, Martínez LM, Borrell V, Marín O. 2013. Contact repulsion controls the dispersion and final distribution of Cajal-Retzius cells. Neuron. 77:457–471.
von Haebler D, Stabel J, Draguhn A, Heinemann U. 1993. Properties of horizontal cells transiently appearing in the rat dentate gyrus during ontogenesis. Exp Brain Res. 94:33–42.
Waterhouse EG, An JJ, Orefice LL, Baydyuk M, Liao GY, Zheng K, Lu B, Xu B. 2012. BDNF promotes differentiation and maturation of adult-born neurons through GABAergic transmission. J Neurosci. 32:14318–14330.
Weeber EJ, Beffert U, Jones C, Christian JM, Forster E, Sweatt JD, Herz J. 2002. Reelin and ApoE receptors cooperate to enhance hippocampal synaptic plasticity and learning. J Biol Chem. 277:39944–39952.
Zhao S, Chai X, Frotscher M. 2007. Balance between neurogenesis and gliogenesis in the adult hippocampus: role for reelin. Dev Neurosci. 29:84–90.